Acta Pharmacologica Sinica

www.nature.com/aps

ARTICLE

Bergapten inhibits NLRP3 inflammasome activation and pyroptosis via promoting mitophagy

Tong Luo[1], Xin Jia[2], Wan-di Feng[3], Jin-yong Wang[2], Fang Xie[1], Ling-dong Kong[2], Xue-jiao Wang[1], Rui Lian[1], Xia Liu[1], Ying-jie Chu[1], Yao Wang[1]✉ and An-long Xu[1]✉

Inhibition of NLRP3 inflammasome activation produces potent therapeutic effects in a wide array of inflammatory diseases. Bergapten (BeG), a furocoumarin phytohormone present in many herbal medicines and fruits, exibits anti-inflammatory activity. In this study we characterized the therapeutic potential of BeG against bacterial infection and inflammation-related disorders, and elucidated the underlying mechanisms. We showed that pre-treatment with BeG (20 μM) effectively inhibited NLRP3 inflammasome activation in both lipopolysaccharides (LPS)-primed J774A.1 cells and bone marrow-derived macrophages (BMDMs), evidenced by attenuated cleaved caspase-1 and mature IL-1β release, as well as reduced ASC speck formation and subsequent gasdermin D (GSDMD)-mediated pyroptosis. Transcriptome analysis revealed that BeG regulated the expression of genes involved in mitochondrial and reactive oxygen species (ROS) metabolism in BMDMs. Moreover, BeG treatment reversed the diminished mitochondrial activity and ROS production after NLRP3 activation, and elevated the expression of LC3-II and enhanced the co-localization of LC3 with mitochondria. Treatment with 3-methyladenine (3-MA, 5 mM) reversed the inhibitory effects of BeG on IL-1β, cleaved caspase-1 and LDH release, GSDMD-N formation as well as ROS production. In mouse model of *Escherichia coli*-induced sepsis and mouse model of *Citrobacter rodentium*-induced intestinal inflammation, pre-treatment with BeG (50 mg/kg) significantly ameliorated tissue inflammation and injury. In conclusion, BeG inhibits NLRP3 inflammasome activation and pyroptosis by promoting mitophagy and maintaining mitochondrial homeostasis. These results suggest BeG as a promising drug candidate for the treatment of bacterial infection and inflammation-related disorders.

Keywords: bergapten; NLRP3 inflammasome; pyroptosis; mitophagy; sepsis; intestinal inflammation

Acta Pharmacologica Sinica (2023) 44:1867–1878; https://doi.org/10.1038/s41401-023-01094-7

INTRODUCTION

The nucleotide-binding domain and leucine-rich repeat-containing (NLR) family pyrin domain-containing protein 3 (NLRP3) inflammasome, which has been implicated in the pathogenesis of inflammatory disorders, can be triggered by a variety of stimuli, including microbial pathogen-associated molecular patterns (PAMPs) or endogenous damage-associated molecular patterns (DAMPs), and therefore needs to be regulated [1, 2]. NLRP3 inflammasome is a multi-protein heteromeric complex existing in the cytoplasm, which is composed of intracellular receptor NLRP3, apoptosis-associated speck-like protein containing a CARD (ASC), and the downstream protease caspase-1. After NLRP3 inflammasome activation, pro-IL-1β, pro-IL-18, and gasdermin D (GSDMD) are cleaved by active caspase-1, generating mature-IL-1β, mature-IL-18 and N-terminal cleavage product (GSDMD-N), thereby triggering a specific form of inflammatory cell death called pyroptosis [3–5]. Additionally, a number of pro-inflammatory factors are released, resulting in an intensified inflammatory response [6]. Thus, blocking NLRP3 inflammasome activation is an effective treatment strategy for treating inflammatory diseases.

Mitochondrial dysfunction induced by NLRP3 stimuli, adenosine 5′-triphosphate disodium (ATP) or nigericin, causes NLRP3 inflammasome activation through the dissipation of mitochondrial membrane potential and the release of mtDAMP, such as mitochondrial reactive oxygen species (ROS) [7–9]. Thus, mitochondrial dysfunction plays the central role in NLRP3 inflammasome activation through multiple mechanisms [1, 10]. Further, studies have demonstrated that mito-TEMPO, a scavenger of mitochondrial ROS, reduces NLRP3 inflammasome activation in macrophage [11]. This suggests that during inflammatory processes, a positive correlation exists between oxidative stress induced by mitochondrial dysfunction and NLRP3 inflammasome activation. Mitophagy eliminates dysfunctional mitochondria and is therefore necessary for maintaining mitochondrial homeostasis and improving the mitochondrial mass [12]. Through early endosomal-dependent mitophagy, the NLRP3 inflammasome's activation could be restricted in macrophages [13]. Furthermore, binding of LC3B to mitochondria and mitophagy is inhibited by pro-IL-1α binding to mitochondrial cardiolipin, and the subsequent accumulation of impaired mitochondria promotes NLRP3 inflammasome activation, leading to increased IL-1β release [14].

[1]School of Life Sciences, Beijing University of Chinese Medicine, Beijing 100029, China; [2]School of Chinese Materia Medica, Beijing University of Chinese Medicine, Beijing 100029, China and [3]Beijing Academy of Traditional Chinese Medicine, Beijing University of Chinese Medicine, Beijing 100029, China
Correspondence: Yao Wang (yaowang@bucm.edu.cn) or An-long Xu (xuanlong@bucm.edu.cn)
These authors contributed equally: Tong Luo, Xin Jia, Wan-di Feng

Received: 12 December 2022 Accepted: 17 April 2023
Published online: 4 May 2023

Therefore, pathophysiological factors such as mitochondrial dysfunction, oxidative stress, and impaired mitophagy contribute to NLRP3 inflammasome activation. Hence, suppressing NLRP3 inflammasome activation and pyroptosis by maintaining mitochondrial homeostasis and promoting mitophagy could be a promising strategy for controlling inflammatory diseases.

Bergapten (5-methoxypsoralen, BeG) is a bioactive coumarin-derived compound extracted from *Cnidium monnieri* (L.) Cusson, *Citrus bergamia* Risso and *Heracleum nepalense* [15–17]. BeG has attracted considerable interest in research owing to its biological activities, including organ protective, neuro-protective, anti-diabetic, anti-cancer, and anti-inflammatory properties [18–20]. BeG also helps in treating asthma by enhancing the activities of superoxide dismutase and catalase. The pro-inflammatory cytokines are suppressed by BeG via the regulation of JAK/STAT pathway [19, 21]. However, as a promising drug candidate for treating inflammatory diseases, the therapeutic efficacy of BeG against bacterial infection and inflammation-related disorders along with the underlying molecular mechanism remain poorly understood.

In this study, we showed that BeG dose-dependently restrained NLRP3 inflammasome activation and pyroptosis, which was accompanied by the reduction in caspase-1 cleavage, mature IL-1β release, and formation of ASC specks. The inhibitory effect of BeG treatment on the NLRP3 inflammasome activation was mediated by mitophagy and improved mitochondrial homeostasis. We also demonstrated that BeG exhibited therapeutic effects in mouse models with bacterial-infected sepsis and intestinal inflammation.

MATERIALS AND METHODS

Antibodies and reagents

ATP salt hydrate (A6419), ultrapure lipopolysaccharides (L4391), Hoechst33342 (B2261) and propidium iodide (P4170) were purchased from Sigma-Aldrich (Munich, Germany); 3-methyladenine (A8353) was from APExBIO (Houston, TX, USA); JC-1 (65-0851-38), MitoTracker Green (M7514), MitoTracker Deep Red (M22426), MitoSOX (M36008) and Penicillin-Streptomycin (15140122) were from Invitrogen (Carlsbad, CA, USA); Pam3CSK4 (tlrl-pms) and nigericin (TLRL-NIG) were from InvivoGen (San Diego, CA, USA); and Bergapten (HY-N0370, $C_{12}H_8O_4$, Mw: 216.19, >99.77%) was from MedChemExpress (Monmouth Junction, NJ, USA). Cytotoxicity LDH (CK12) assay and cell counting kit-8 (CK04-100) were obtained from Dojindo (Kumamoto, Japan). Mouse IL-1β enzyme-linked immunosorbent assay kits (KE10003-96T) and mouse tumor necrosis factor (TNF-α) ELISA kits (KE10002-96T) were purchased from Proteintech (Chicago, IL, USA). Evo M-MLV RT-PCR Kit (AG11601) and SYBR Green Premix *Pro Taq* HS qPCR Kit (AG11701) were from Accurate Biology (Changsha, China). Dulbecco's Modification of Eagle's Medium (C11995500BT) and Fetal Bovine Serum (1600044) were purchased from Gibco (Carlsbad, CA, USA). Murine M-CSF (315-02) was from PeproTech (Rocky Hill, NJ, USA). Anti-GSDMD (1:1000, ab209845), anti-caspase-1 (1:2000, ab179515), anti-LC3B (1:1000, ab48394) antibodies were obtained from Abcam (Cambridge, MA, USA). Anti-NLRP3 (1:1000, AG-20B-0014-C100) and Anti-ASC (1:1000, AG-25B-0006-C100) antibodies were obtained from Adipogen (San Diego, CA, USA). *Escherichia coli* (ATCC 11303) was purchased from ATCC (Manassas, VA, USA), and *Citrobacter rodentium* was supplied by Prof. Chen Dong (Tsinghua University, Beijing, China).

Mice

Male C57BL/6J mice (age, 8 weeks) were obtained from SPF Biotechnology Co., Ltd. and allowed to acclimatize for 1 week in a specific pathogen-free (SPF) environment before the experimental procedures (Approval No. BUCM-4-2022041304-2017).

Cell culture

For the isolation of BMDMs, femur and tibias were removed from wild-type mice. Using a 5 mL syringe needle, a small hole was made at the bottom of a 0.6 mL microcentrifuge tube. The epiphysis was carefully cut off and the isolated tibia and femur were placed in a 0.6 mL microcentrifuge tube nested in a 1.5 mL microcentrifuge tube. Marrow was then transferred to the bottom tube by centrifugation at 10,000 × *g* for 30 s. Primary BMDMs were cultured for seven days at 37 °C in DMEM supplemented with 20% FBS, M-CSF (25 ng/mL), and 1% penicillin-streptomycin (P/S). The medium was supplemented on day 3 and replaced on day 5. Immortalized BMDM (iBMDM) cells and mouse macrophage cell line J774A.1 were cultured in DMEM supplemented with 10% FBS and 1% P/S.

Inflammasome activation

For NLRP3 inflammasome stimulation, J774A.1 cells were pre-treated with BeG (20 μM) for 2 h and primed with LPS (500 ng/mL) for 4 h before NLRP3 stimulus was added: nigericin (20 μM) or ATP (4 mM) for 1 h unless otherwise specified. To activate the canonical NLRP3 inflammasome, BMDMs or iBMDM were pre-treated with BeG (20 μM) for 2 h and primed with LPS (100 ng/mL for BMDM, 500 ng/mL for iBMDM) for 4 h before NLRP3 stimulus was added: nigericin (10 μM) for 1 h or ATP (4 mM) for 1 h. To activate non-canonical NLRP3 inflammasome, BMDMs were primed with Pam3CSK4 (100 ng/mL) for 4 h. The medium was replaced and a dose of 1 μg/mL LPS was transfected for 16 h with FuGENE HD transfection reagent. To study the effects of BeG treatment on NLRP3 priming, BMDMs were incubated with BeG (20 μM) for 2 h before LPS (500 ng/mL) stimulation for 4 h. THP-1 was incubated with BeG (20 μM) and LPS (500 ng/mL) for 4, 8, and 12 h.

Cell death assays

Lactate dehydrogenase (LDH) release assay and propidium iodide (PI) incorporation were used to analyze cell death. The culture medium was analyzed for LDH release as directed by the assay kit's manufacturer. To examine the inflammatory cell death, the cells were stained for 10 min with PI (4 μg/mL) and Hoechst33342 (5 μg/mL). Images of pyroptotic cells were acquired using an INCell Analyser 2500 with High Content Analysis (GE Healthcare, Pittsburgh, PA, USA).

Enzyme-linked immunosorbent assay (ELISA)

Conditioned media or serum was collected and mouse IL-1β and TNF-α was quantified using the respective ELISA kits following the manufacturer's instructions (Proteintech, Chicago, IL, USA).

Immunoblotting

As described previously, an equal volume of medium was collected and precipitated for detecting secreted caspase-1 p10 in J774A.1 cells or BMDMs [22, 23]. The protein samples were separated by SDS-PAGE electrophoresis, followed by their electrophoretic transfer onto nitrocellulose filter membranes. After overnight incubation at 4 °C with primary antibodies, the membranes were incubated with appropriate secondary horseradish peroxidase (HRP) conjugated antibodies for 1 h. Protein expression was assessed using a Tanon (Shanghai, China) 5200 automatic chemiluminescence image analysis system.

Flow cytometric analyses

The mitochondrial mass of J774A.1 cell was detected by staining with MitoTracker Deep Red (150 nM) and MitoTracker Green (100 nM) for 30 min. Mitochondria-associated ROS levels of J774A.1 cells were measured at 37 °C by staining cells with 5 μM MitoSOX for 30 min. J774A.1 cells were then washed and resuspended in a 500 μL PBS containing 2% FBS for fluorescence-activated cell sorting (FACS).

Table 1. Primer sequence (forward and reverse).

Gene	Forward primer	Reverse primer
IL1B	5′-TTCGACACATGGGATAACGAGG-3′	5′-TTTTTGCTGTGAGTCCCGGAG-3′
IL6	5′-ACTCACCTCTTCAGAACGAATTG-3′	5′-CCATCTTTGGAAGGTTCAGGTTG-3′
Il1b	5′-CTGTGACTCATGGGATGATGATG-3'	5′-CGGAGCCTGTAGTGCAGTTG-3'
Il6	5′-CTGCAAGAGACTTCCATCCAG-3′	5′-AGTGGTATAGACAGGTCTGTTGG-3′
Tnf	5′-CCTGTAGCCCACGTCGTAG-3′	5′-GGGAGTAGACAAGGTACAACCC-3′
Tgfb1	5′-CTCCCGTGGCTTCTAGTGC-3′	5′-GCCTTAGTTTGGACAGGATCTG-3′
D-loop	5′-AATCTACCATCCTCCGTGAAACC-3′	5′-TCAGTTTAGCTACCCCCAAGTTTAA-3′
Tert	5′-CTAGCTCATGTGTCAAGACCCTCTT-3'	5′-GCCAGCACGTTTCTCTCGTT-3'

Relative gene expression levels were analyzed by relative quantitative $2^{-\Delta\Delta CT}$ method.

Confocal microscopy

To observe the formation of ASC specks, BMDMs were fixed for 20 min in 4% paraformaldehyde and permeabilized with 0.5% Triton X-100 for 20 min. Nonspecific binding was blocked using 10% goat serum. Cells were incubated with anti-ASC (1:100) at 4 °C, followed by incubation with Alexa Fluor 488 for 1 h and Hoechst 33342 for 10 min. To detect the co-localization of LC3 and mitochondria, BMDMs were incubated with anti-LC3B (1:150), followed by staining with Alexa Fluor 647 and MitoTracker Green (100 nM). JC-1 staining (2 μM) was used to measure the mitochondrial membrane potential. Confocal images were immediately captured using an Olympus confocal microscope (FV3000, Tokyo, Japan) and rendered using vendor-supplied software.

Transmission electron microscope

The BMDMs were treated as described above, following which the samples were dehydrated and embedded in acrylic resin. Ultrathin samples were mounted on nickel grids, stained with lead citrate and uranyl acetate, and rinsed with distilled water. Images were acquired on an electron microscope and rendered using vendor-supplied software.

DNA and RNA isolation and real-time qPCR

The experiments were conducted following the protocols described previously [24]. DNeasy kits (Qiagen) were used for the purification of cellular DNA. To quantify the mitochondrial DNA (mtDNA)/nuclear DNA (nDNA) ratio, one gene from the mitochondrial genome (*D-loop*) and one from the nuclear genome (*Tert*) were amplified by qPCR. Whole-cell RNA was extracted from BMDMs or THP-1 cells using the TRIzol reagent. RNA was reverse-transcribed with the Evo M-MLV RT-PCR Kit for cDNA synthesis. cDNA was amplified by qPCR with SYBR Green Premix *Pro Taq* HS qPCR Kit. Primer sequences are listed in Table 1.

RNA sequencing and bioinformatics analyses

After LPS-ATP stimulation, the cellular RNA was extracted from BMDMs using the TRIzol reagent. Samples that passed the basic quality metrics were used for RNA-Seq analysis. The sequencing quality was assessed with FastQC (v0.11.5) and low-quality data were filtered using NGSQC (v2.3.3). The gene expression analyses were carried out by StringTie (v1.3.3b). DESeq (v1.28.0) was used to analyze the differentially expressed genes (DEGs) between samples. Parameters for identifying DEGs were ≥2-fold differences ($|\log_2 FC| \geq 1$, FC: fold change in expression) in the transcript abundance and $P \leq 0.05$. The volcano plot and heatmap were generated using R 4.0.3 software. Gene Ontology (GO) functional enrichment analysis was conducted via the R package 'clusterProfiler'. Gene set enrichment analysis (GSEA) was performed on the GSEA 4.1.0 software with gene sets sourced from the MSigDB database.

E. coli-induced bacteremia model

For *E. coli*-induced septic shock, mice ($n = 12$) were injected intraperitoneally (i.p.) with BeG (50 mg/kg) or PBS 24 h and 1 h before injecting *E. coli* (1×10^{11} CFU/kg). The mortality rate of mice was monitored regularly. To induce inflammatory cytokine secretion, mice ($n = 5$) were i.p. injected with BeG (50 mg/kg) or PBS for 24 h and 1 h before injecting *E. coli* (5×10^{10} CFU/kg). Serum samples were collected 6 h post-infection and cytokine levels were measured using ELISA. The mice were sacrificed. The lungs were removed for haematoxylin and eosin (H&E) staining or Western blot, and colon and liver were removed for H&E staining.

Mouse model of *C. rodentium* infection

For *C. rodentium* infection, mice ($n = 5$) were intragastrically (i.g.) infected with 25×10^{10} CFU·kg^{-1}·d^{-1} bacteria 1 h after BeG administration (50 mg/kg). Body weight was measured every 2 days. On the ninth day, the mice were sacrificed, and the colon and jejunum were removed for H&E staining. The viscera indices (spleen, kidney, and liver) were also measured. Liver, kidneys, and mesenteric lymph nodes were removed and homogenized to measure the bacterial burden.

Haematoxylin and eosin staining

After the mice were anaesthetized with isoflurane and sacrificed, visceral tissues were isolated and fixed in 4% paraformaldehyde. The tissue specimens were subsequently removed and embedded in paraffin. Sample sections were stained with H&E solution.

Statistical analysis

Data were analyzed using the GraphPad Prism 8.0.2 software. Statistical significance for experiments with multiple groups and a single independent variable was tested with one-way analysis of variance (ANOVA) followed by Bonferroni post-test. Two-way ANOVA was used for analysis of multiple groups with multiple independent variables. For the survival analysis, a log-rank test was used. The mean represents the central tendency and error bars represent the standard deviation (SD) in all the graphs.

RESULTS

Bergapten attenuates NLRP3 inflammasome activation

Although NLRP3 inflammasome is essential for immunity against pathogenic infections, dysregulated activation of NLRP3 inflammasome can lead to various inflammatory diseases [25]. Considering that BeG (Fig. 1a) has been proven to be a natural anti-inflammatory agent, we examined its effects on NLRP3 inflammasome activation. Firstly, the viability of J774A.1 cells is measured using the CCK-8 assay and concentrations of BeG (5, 10, and 20 μM) are selected for further experiments based on their low cytotoxicity (Fig. 1b). Next, the level of caspase-1 cleavage in

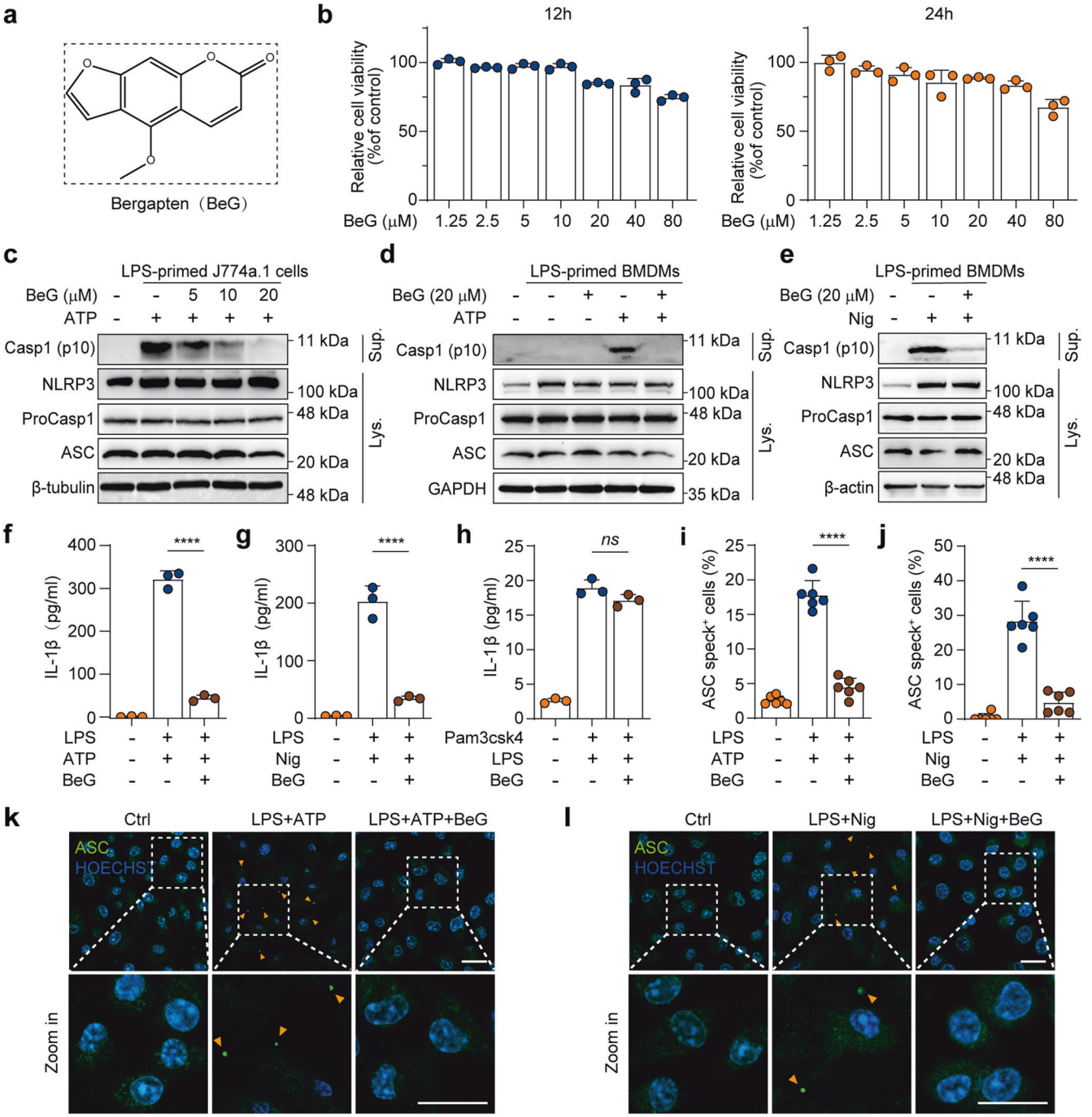

Fig. 1 Bergapten (BeG) attenuates nucleotide-binding domain and leucine-rich repeat-containing (NLR) family pyrin domain-containing protein 3 (NLRP3) inflammasome activation. a Molecular structure of BeG. **b** Cytotoxicity of J774A.1 cells after 12 and 24 h of BeG treatment ($n = 3$ per group). **c–e** Western blotting analysis of NLRP3, pro-caspase1, apoptosis-associated speck-like protein containing a CARD (ASC) and NLRP3 inflammasome activation-related protein (Casp1-p10) from the cell (J774A.1 and bone marrow-derived macrophages [BMDMs]) lysates and culture supernatants. **f–h** Effect of BeG treatment on interleukin-1β (IL-1β) production in the culture supernatants of BMDMs ($n = 3$ per group). **i–l** Images of immunofluorescence showing the subcellular distribution of ASC (green). Nuclei (blue) are shown by Hoechst 33342 (arrowheads mark ASC specks); scale bar: 20 μm. Quantification of ASC specks was done from six random fields (one field per well) ($n = 6$ per group). Data shown as mean ± SD (****$P < 0.0001$; ns not significant).

the conditioned media is measured. Immunoblotting results reveal that BeG treatment inhibits cleaved caspase-1 release in both BMDMs and J774A.1 cells (Fig. 1c–e). In addition, BeG treatment attenuates IL-1β secretion under nigericin and ATP stimulation, but this does not affect non-canonical NLRP3 activation by intracellular LPS stimulation, as determined by ELISA (Fig. 1f–h). ASC is an important component in the formation of intracellular supramolecular complexes of inflammasomes. Upon NLRP3 activation, ASC proteins form large spherical structures (referred to as 'specks') in the perinuclear region, by self-association before the activation of downstream signaling cascade [26]. Our results demonstrate that BeG substantially decreases the formation of ASC specks in LPS-primed BMDMs upon ATP or nigericin stimulation (Fig. 1i–l).

It takes two steps to activate the NLRP3 inflammasome: priming and activation. The first step (priming) enables the cell to transcribe the NLRP3 gene and other pro-inflammatory genes, whereas the second step occurs following the recognition of various PAMPs or DAMPs and induces full activation and formation of the NLRP3 inflammasome [1, 25]. Based on the above findings that BeG inhibits NLRP3 inflammasome activation, we suspected that priming is regulated by BeG. To evaluate the effect of BeG on the priming step, BMDMs are stimulated with LPS. Remarkably, upon LPS stimulation, increased messenger RNA (mRNA) expression levels of *Il1b* and *Il6* are detected by qPCR. However, transcription levels of *Il1b* and *Il6* genes in BMDMs treated with BeG does not show changes upon LPS stimulation (Supplementary Fig. S1a, b). Consistently, similar results were obtained from LPS-stimulated THP-1 cells, indicating that BeG that does not inhibit the gene expression levels of *IL1B* and *IL6* (Supplementary Fig. S1c, d). Moreover, BeG does not suppress the expression of NLRP3, caspase-1, and ASC, upon LPS stimulation, as determined by Western blotting (Supplementary Fig. S1e). Therefore, these findings indicate that BeG inhibited NLRP3 inflammasome activation and the effects of BeG on NLRP3 inflammasome activation were independent of inhibition of the priming step.

BeG inhibits pyroptosis

In addition to the caspase-1-dependent release of pro-inflammatory cytokines, NLRP3 inflammasome activation can result in GSDMD-mediated pyroptosis [27]. Considering that BeG significantly suppressed IL-1β and formation of ASC speck, we sought to investigate the effects of BeG on pyroptosis. Results demonstrate that upon ATP stimulation, BeG dose-dependently decreases the ratio of PI-positive J774A.1 cells (Fig. 2a, b). BeG also attenuated cell death in LPS-primed BMDMs in response to ATP or poly (I:C) (Fig. 2c, d, Supplementary Fig. S2a). Next, an LDH release assay was performed to quantify pyroptosis. BeG decreases LDH release in response to either nigericin or ATP (Fig. 2e, f). Some characteristic morphological changes, including cell swelling, cessation of movement, and development of ballooning cell membranes that disintegrate abruptly to yield an atrophied corpse, are observed in LPS-primed BMDMs stimulated with either nigericin or ATP (Fig. 2g–j). Consistent with the reduction in LDH release, these morphological changes are reversed by BeG treatment (Fig. 2g–j). Moreover, BeG blocks the formation of GSDMD-N which results in release of pro-inflammatory factors by promoting membrane rupture in J774A.1, BMDMs, and iBMDM cells, with ATP or nigericin stimulation (Fig. 2k–m, Supplementary Fig. S2b). These results demonstrated that BeG suppresses pyroptosis induced by NLRP3 stimuli, ATP, or nigericin, suggesting its potential role in suppressing the inflammatory response.

BeG improves mitochondrial homeostasis in response to NLRP3 inflammasome activation

To determine which genes were significantly up- or down-regulated by BeG during NLRP3 inflammasome activation, LPS-primed BMDMs were stimulated with ATP with or without BeG pre-treatment and subjected to RNA sequencing analysis. As shown in Supplementary Fig. S3a, 492 DEGs are identified between LPS + ATP + BeG and LPS + ATP groups, with 129 up-regulated and 363 down-regulated genes.

Intriguingly, we found that genes upregulated in the BeG treatment group, as compared with the NLRP3 inflammasome activated group are involved in mitochondrial function such as oxidative phosphorylation (*Gpx3*, *prdx1*, *Txnrd1*, etc), mitochondrial metabolism (*Cox17*, *Uqcrb*, *Vadc1*, etc), and mitophagy (*Becn1*, *Atg4b*, *Atg5*, etc). In contrast, oxidative stress-related genes (*Nox1*, *Nos2*, *Cdkn1a*, etc) are down-regulated (Fig. 3a). Furthermore, GSEA results demonstrate that DEGs are up-regulated in biological process (BP) of mitochondrial translation but negatively enriched in BP of oxidative damage by BeG treatment with normalized enrichment scores (NES) of 2.02 and −1.50, respectively (Fig. 3b). GO enrichment analysis focusing on BP is performed to identify DEGs that are primarily enriched in the immune response and ROS metabolism (Supplementary Fig. S3b).

Accumulated evidence has revealed that mitochondrial damage and mitochondrial ROS generation are upstream events in the NLRP3 inflammasome activation [8, 28, 29]. The bioinformatics analysis results clearly illustrated BeG treatment may improve mitochondrial homeostasis in response to NLRP3 inflammasome activation. To validate this speculation, TEM is employed to visualize mitochondrial structural features. Swollen mitochondria with severe disruption are noted in BMDMs treated with LPS and ATP, whereas BeG treatment significantly improves mitochondrial morphology (Fig. 3c). To further investigate the potential effects of BeG treatment on mitochondrial activity upon stimulation, the mitochondrial membrane potential (MMP) was determined with JC-1 or MitoTracker Green (labeling total mitochondria) and MitoTracker Deep Red (labeling respiratory mitochondria). Results show that the JC-1 aggregates (red)/monomer (green) ratio is much lower in LPS-primed BMDMs stimulated with ATP, indicating that MMP is significantly decreased, whereas BeG treatment significantly elevates MMP (Fig. 3d, e). Consistent with this observation, the ratio of dysfunctional mitochondria increases in LPS-primed BMDMs in response to either ATP or nigericin, while BeG treatment significantly reverses this change, indicating the protective effects of BeG on mitochondrial function (Fig. 3f–h). Owing to the lack of nucleosomes and DNA repair mechanisms, mtDNA is highly vulnerable to damage, which can result in its depletion [30]. Quantification of mtDNA copy number is an indicator of mitochondrial mass and is a good biomarker for disease progression [31]. Thus, mtDNA levels were detected by qPCR. As expected, LPS and ATP stimulation or CCCP treatment results in lower mtDNA levels; however, BeG treatment significantly reverses the reduction in mtDNA levels (Fig. 3i, j). Mitochondria are exquisitely complex regulators of cytosolic homeostasis, and stress conditions like membrane damage can markedly induce mitochondrial ROS production [32, 33]. As detected by fluorescence of MitoSOX, mitochondrial superoxide anion radical ($O_2^{\bullet\,-}$) increases in by J774A.1 cells with LPS and ATP stimulation, indicating enhanced mitochondrial ROS production. In contrast BeG treatment significantly decreases the mitochondrial ROS levels (Fig. 3k, l). Therefore, our data demonstrates that treatment with BeG improves mitochondrial integrity and function in response to NLRP3 inflammasome activation.

BeG promotes mitophagy to inhibit NLRP3 inflammasome activation

Bioinformatic analysis suggests that effect of BeG treatment in maintaining mitochondrial homeostasis is associated with mitophagy (Fig. 3a, b). Mitophagy is an important quality control mechanism for mitochondria that eliminates dysfunctional mitochondria to maintain cellular homeostasis [32, 34]. Therefore, we investigated whether BeG treatment affected mitophagy during inflammasome activation. During the formation of autophagosomes, LC3-I protein is converted to the autophagic vesicle-associated form (LC3-II), which is an important marker of autophagic activity within cells [35]. Upon NLRP3 activation, treatment with BeG enhances the protein level of LC3-II in BMDMs (Fig. 4a). The degree of co-localization of mitochondria and LC3 increases significantly after BeG treatment. Additionally, 3-MA, which is an inhibitor of autophagy suppresses this effect (Fig. 4b). Thus, the inhibition of IL-1β release and its mRNA expression by BeG treatment is reversed by 3-MA treatment (Fig. 4c–g). Consistent with this, BeG-mediated inhibition of cleaved caspase-1 release, LDH release, and GSDMD-N formation is reversed by 3-MA treatment (Fig. 4h–j). 3-MA also increases the

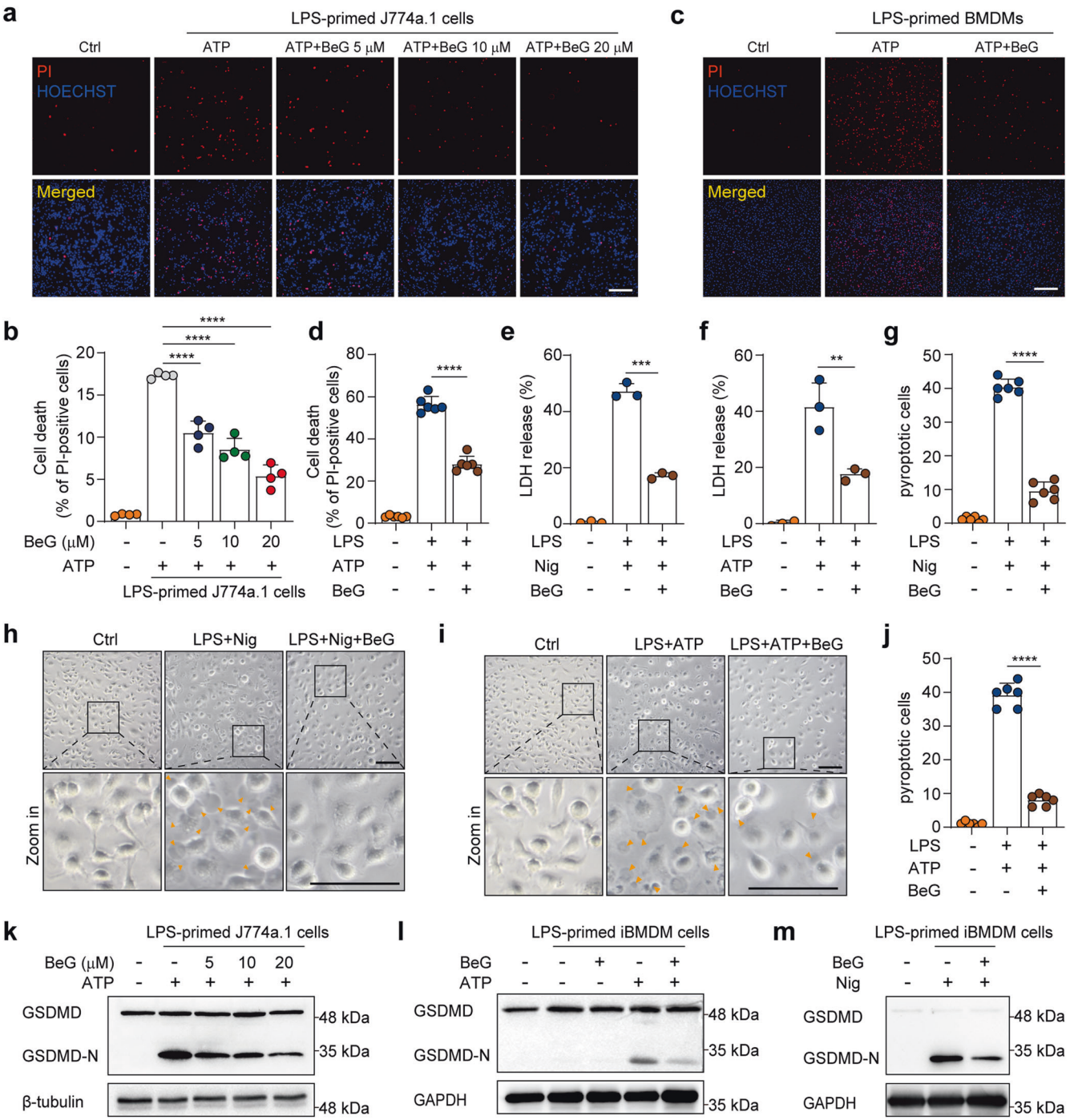

Fig. 2 BeG inhibits pyroptosis. a, **b** Propidium iodide (PI) and Hoechst 33342 stained J774A.1 cells treated with BeG for 2 h, lipopolysaccharides (LPS) for 4 h, and nigericin for 1 h; scale bar 250 μm. Percentages of PI-positive cells relative to all cells were quantified by counting four randomly chosen fields (one field per well) ($n = 4$ per group). **c**, **d** PI and Hoechst 33342 stained BMDMs cells; scale bar 200 μm. Percentages of PI-positive cells relative to all are quantified by counting six randomly chosen fields (one field per well) ($n = 6$ per group). **e**, **f** Effects of BeG treatment on lactate dehydrogenase (LDH) release of LPS-primed BMDMs stimulated with nigericin or adenosine 5′-triphosphate disodium (ATP) in culture supernatants ($n = 3$ per group). **g–j** Bright-field images of LPS-primed BMDMs upon ATP or nigericin stimulation with or without BeG pre-treatment (arrowheads mark pyroptotic cells). The percentage of pyroptotic cells. Scale bar is 100 μm. A total of six randomly chosen fields were counted to quantify the number of pyroptotic cells ($n = 6$ per group). **k** J774A.1 cells were pre-treated with BeG for the indicated concentrations before LPS-ATP stimulation, followed by immunoblotting. **l**, **m** Immunoblot analysis of N-terminal cleavage product of gasdermin D (GSDMD-N) expression in LPS-primed immortalized BMDM (iBMDM) cells treated with nigericin or ATP with or without BeG pre-treatment. Data shown as mean ± SD (**$P < 0.01$, ***$P < 0.001$, ****$P < 0.0001$).

frequency of MitoSOX-positive cells and enhances the fluorescence intensity of relative ROS expression in J774a.1 cell (Fig. 4k, l). These results suggest that BeG suppresses NLRP3 inflammasome activation by promoting mitophagy.

BeG protects against sepsis induced by *E. coli*

To elucidate the physiological function of BeG treatment in inflammatory diseases mediated by the NLRP3 inflammasome, a mouse model of *E. coli*-induced sepsis is used to determine the effect

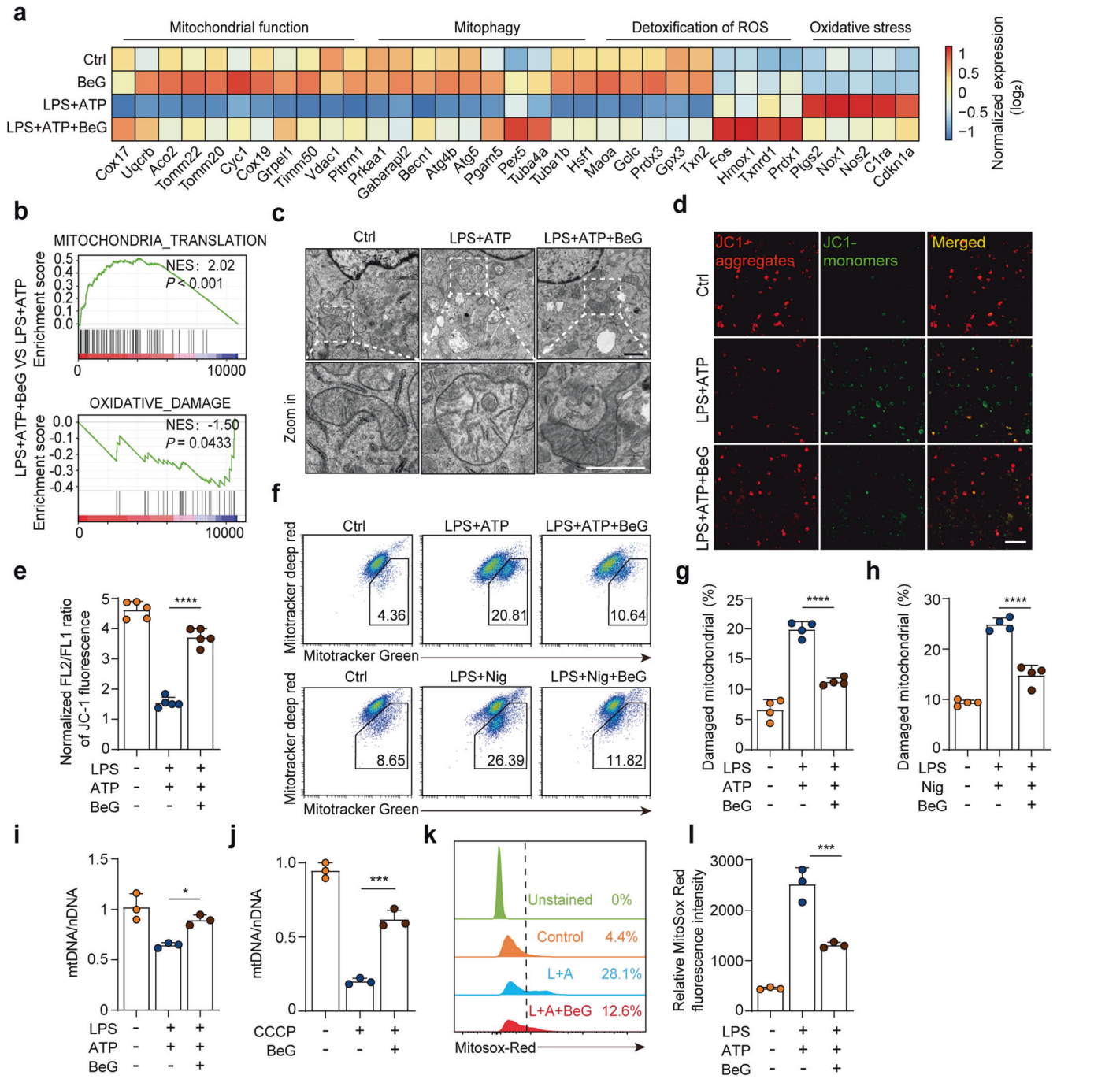

Fig. 3 BeG improves mitochondrial homeostasis in response to NLRP3 inflammasome activators. a RNA-seq heat map showing the relative mRNA levels of genes associated with mitochondrial function, mitophagy, detoxification of ROS, and oxidative stress pathway for LPS + ATP + BeG and LPS + ATP groups. **b** Gene set enrichment analysis (GSEA) of significantly up-regulated genes in the LPS + ATP + BeG group as compared to the LPS + ATP group. **c** Analysis of morphology of mitochondria in BMDMs using transmission electron microscope; scale bar 1 μm. **d**, **e** Mitochondrial membrane potential in BMDMs was analyzed by the JC-1 using confocal microscopy ($n = 5$ per group). Scale bar 25 μm. **f–h** J774A.1 cells were stained with Mitotracker Green (labeling total mitochondria) and Mitotracker Deep Red (labeling respiratory mitochondria) after LPS-ATP stimulation and then analyzed by flow cytometry ($n = 4$ per group). **i, j** qPCR analysis of the mtDNA/ nDNA ratio in BMDMs ($n = 3$ per group). **k, l** J774A.1 cells were pre-treated with BeG, stimulated with LPS and ATP, stained with MitoSOX and analyzed by flow cytometry ($n = 3$ per group). Data shown as mean ± SD (*$P < 0.05$, ***$P < 0.001$, ****$P < 0.0001$).

of BeG treatment in vivo (Fig. 5a). Administration of BeG improve mouse survival after *E. coli* infection compared to that in *E. coli* group (Fig. 5b). Furthermore, IL-1β levels sharply increase in the serum after bacterial infection. Although, BeG administration results in a significant decrease in IL-1β secretion, but no significant inhibitory effect is observed on serum TNF-α levels (Fig. 5c, d). H&E staining also indicates that BeG treatment significantly alleviates *E. coli*-induced overt infiltration of inflammatory cells in the lungs, colon, and liver of mice (Fig. 5e–g). To further clarify the pharmacological function of BeG on *E. coli*-induced sepsis, we analyzed the NLRP3-GSDMD pathway and LC3 in lungs. The results showed that *E. coli* increases the expression of NLRP3, cleaved caspase-1 and GSDMD-N (Fig. 5h).

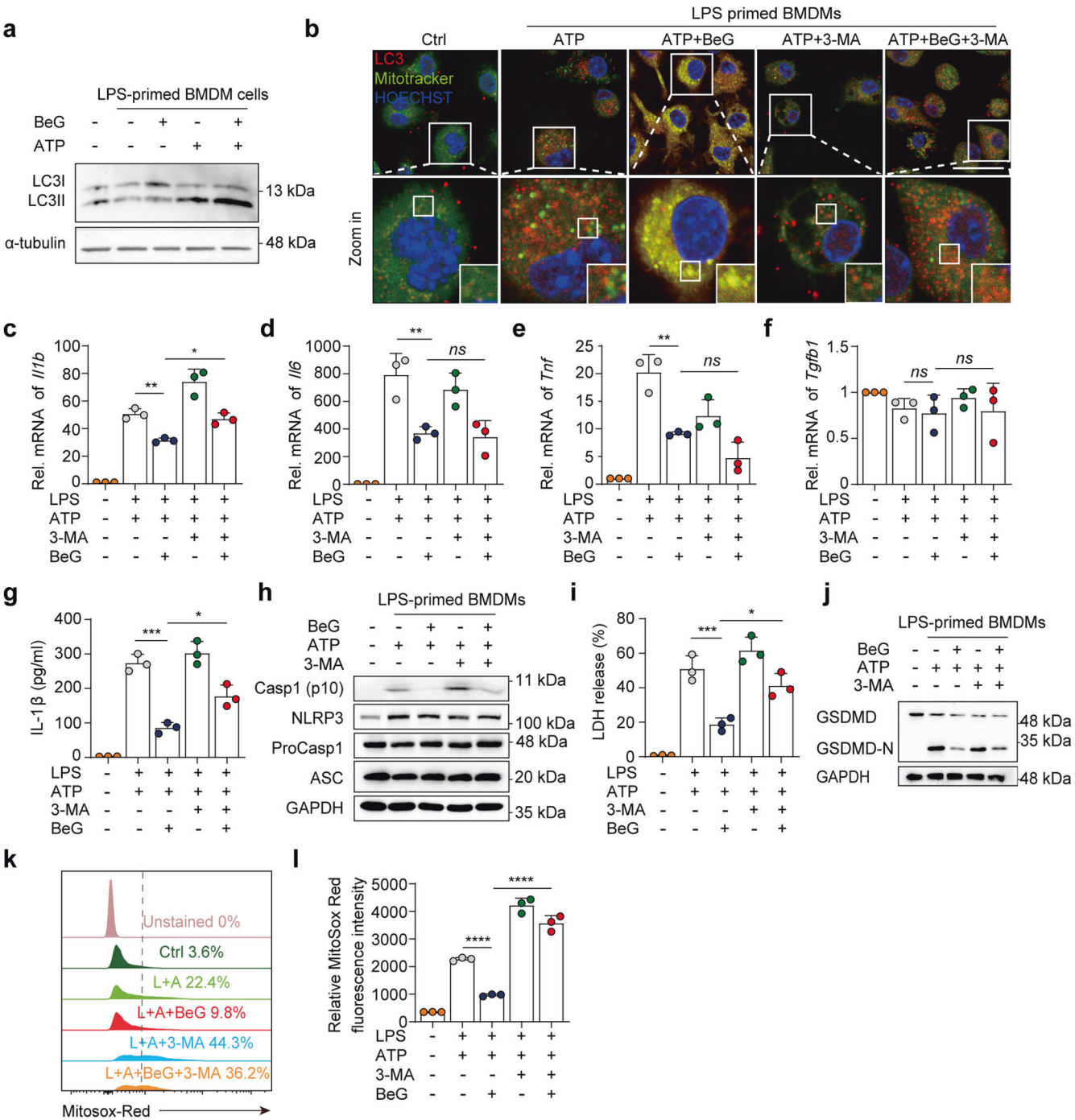

Fig. 4 BeG promotes mitophagy to inhibit NLRP3 inflammasome activation. a Western blotting analysis of LC3B in BMDMs treated as indicated in the image. **b** Confocal microscopy of BMDMs pre-treated with BeG stimulated with LPS and treated with ATP, stained for LC3 with Mitotracker. Scale bars, 25 μm. **c**–**f** Effects of BeG, LPS, 3-methyladenine (3-MA, 5 mM), and ATP stimulation on level of *Il1b*, *Il6*, *Tnf*, *Tgfb1* microRNA (mRNA) in BMDMs ($n = 3$ per group). **g** Measurement of IL-1β in BMDMs ($n = 3$ per group). **h** Immunoblot analysis of protein levels of core NLRP3 inflammasome components (NLRP3, ProCasp1, and ASC) and NLRP3 inflammasome activation-related proteins (Casp1-p10) from the BMDMs lysates and culture supernatants. **i** LDH release in culture supernatants ($n = 3$ per group). **j** Immunoblot analysis of GSDMD-N formation in BMDMs. **k**, **l** J774A.1 cells were pre-treated with BeG, treated with LPS with or without 3-MA (5 mM), stimulated by ATP, and then stained with MitoSOX and analyzed by flow cytometry ($n = 3$ per group). Data shown as mean ± SD (*$P < 0.05$, **$P < 0.01$, ***$P < 0.001$, ****$P < 0.0001$; ns not significant).

Pre-treatment with BeG significantly inhibits *E. coli*-induced expression of cleaved caspase-1 and GSDMD-N in lung (Fig. 5h). Simultaneously, pre-treatment with BeG also leads to increase of LC3 II (Fig. 5h), suggesting that BeG may also promote autophagy and inhibit NLRP3 inflammasome activation in mice. Collectively, these data demonstrate that pre-treatment with BeG exerted protection against bacterial infections by alleviating the inflammatory immune response and repressing NLRP3 inflammasome activation.

BeG ameliorates *C. rodentium*-induced intestinal inflammation

We further investigated whether BeG protects mice from *C. rodentium*-associated intestinal inflammation, which is

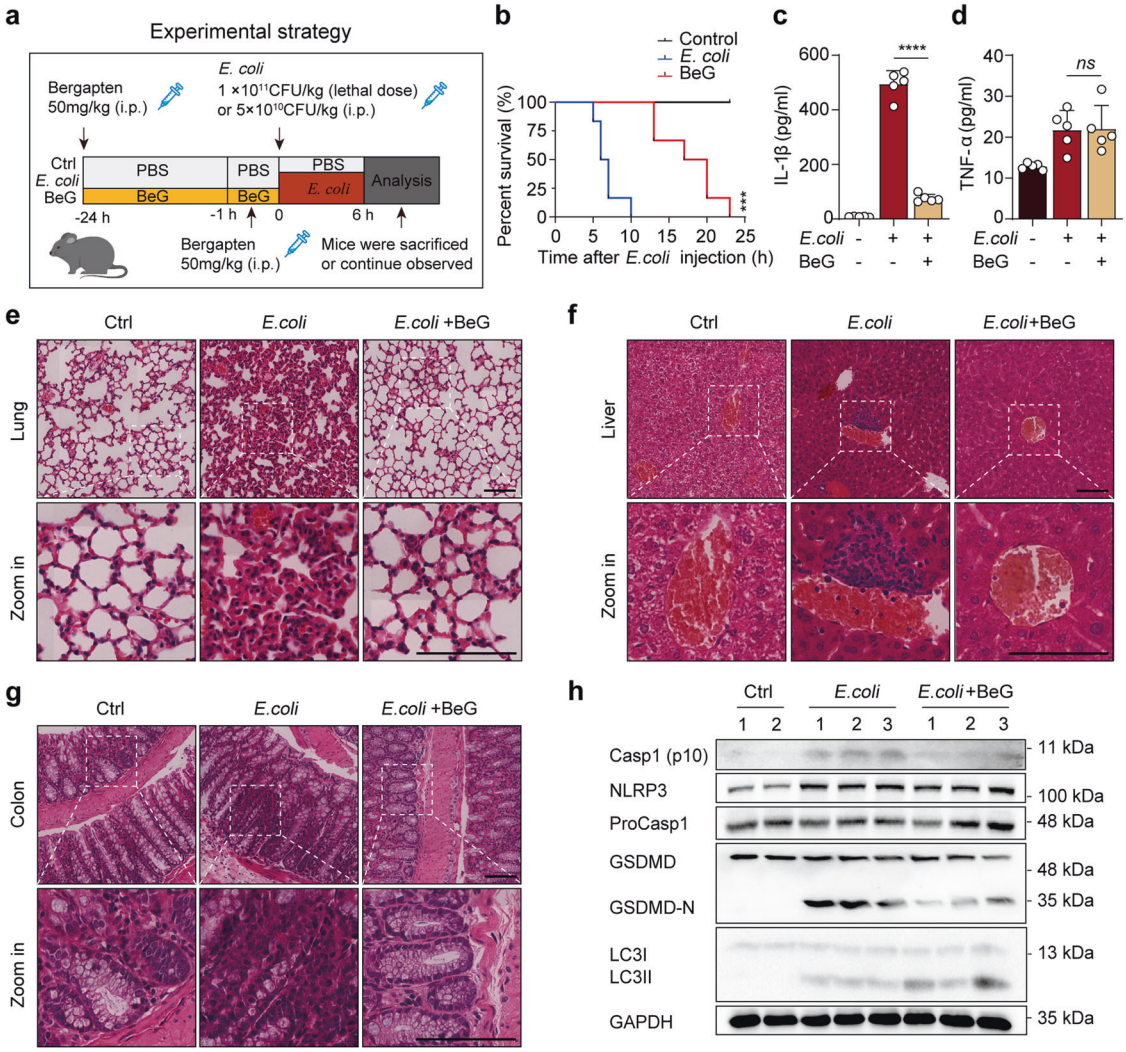

Fig. 5 BeG protects against sepsis induced by *E. coli*. **a** Schematic of the experimental strategy. **b** Survival of mice intraperitoneally injected with *E. coli* (1×10^{11} CFU/kg) with or without BeG pre-treatment (50 mg/kg, $n = 12$ per group). **c**, **d** Cytokine (IL-1β, tumor necrosis factor [TNF-α]) concentrations in the serum ($n = 5$ per group). **e**–**g** Representative microscopic pictures of lung, liver and colon H&E staining. **h** Western blot analysis of the expression of NLRP3, ProCasp1, GSDMD, Casp1-p10, and LC3 protein in the lung. Scale bar 100 μm. Data shown as mean ± SD (***$P < 0.001$, ****$P < 0.0001$; ns not significant).

mediated by the non-canonical NLRP3 inflammasome (Fig. 6a). *C. rodentium* infection resulted in significant weight loss and colon length shortening, which are reversed by BeG treatment, indicating its protective effects (Fig. 6b, c). Following the infection, the bacteria grow rapidly inside the host. Thus, we determine the bacterial loads in different organs. As shown in Fig. 6d–f, BeG treatment leads to lower bacterial loads than that in the model group. Furthermore, the results exhibit that *C. rodentium* infection increases the spleen and kidney index and these pathological changes are relieved by BeG administration (Fig. 6g–i). H&E staining indicate that mice infected with *C. rodentium* show inflammatory cell infiltration and severe barrier breakdown of the colon and jejunum, whereas BeG treatment substantially attenuates these pathological phenotypes (Fig. 6j, k). Together, these results demonstrate that inflammation induced by *C. rodentium* is inhibited by BeG, in vivo.

DISCUSSION

BeG is a natural psoralen derivative present in a wide range of medicinal plants which has shown substantial anti-inflammatory and immunomodulatory actions, however, its clinical application is limited because of the poorly understood mechanism of action. The NLRP3 inflammasome plays a pivotal role in host defence against pathogens, however, abnormal NLRP3 inflammasome activation leads to uncontrolled infection and metabolic, autoimmune, and neurodegenerative disorders [36, 37]. The pyroptosis execution protein GSDMD, which is expressed in the bone marrow, colon, intestines, spleen, kidney, and other tissues, is cleaved by NLRP3 inflammasome-activated caspase-1 or intracellular LPS-activated caspase-4/5/11 [38]. Consequently, strict control of NLRP3 inflammasome assembly and signaling is important for the immune system to initiate inflammatory responses and antimicrobial activity while avoiding excessive tissue damage [39]. In this study, we demonstrated that BeG treatment could significantly inhibit NLRP3 inflammasome activation, cytokine release, and GSDMD-N formation in macrophage and pyroptosis, suggesting that BeG can be used as a novel candidate to treat NLRP3-driven diseases. Additionally, our results suggest that the effects of BeG on NLRP3 inflammasome activation do not rely on inhibition of the priming step.

Thus far, the exact mechanism involved in NLRP3 inflammasome activation and the contribution of different organelles remains unclear [40]. One hypothesis regarding the NLRP3

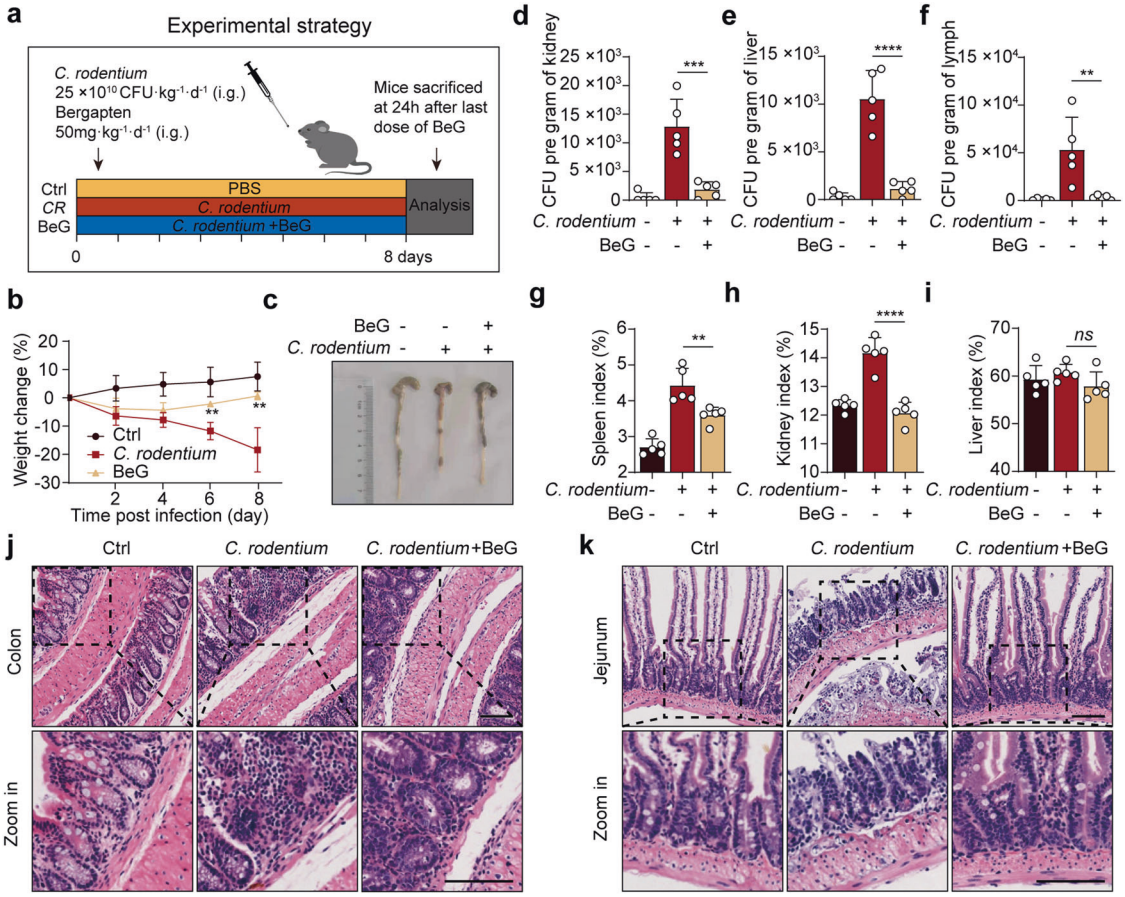

Fig. 6 BeG treatment ameliorates *C. rodentium*-induced intestinal inflammation. a Schematic of the experimental strategy. **b** Body weight change ($n = 5$ per group). **c** Representative pictures of colon length and colon gross appearance. **d**–**f** Number of bacteria in kidney, liver, and mesenteric lymph nodes ($n = 5$ per group). **g**–**i** Effects of BeG treatment on viscera (spleen, kidney, and liver) index of *C. rodentium*-induced intestinal inflammation model ($n = 5$ per group). **j**, **k** Representative microscopic pictures of colon and jejunum H&E staining. Scale bars 100 μm. Data shown as mean ± SD (**$P < 0.01$, ***$P < 0.001$, ****$P < 0.0001$; ns not significant).

inflammasome activation mechanism is mitochondrial dysfunction [41, 42]. As described earlier, NLRP3 inflammasome activation is usually accompanied by the disruption of MMP and ROS generation. A lower concentration of CCCP that partially impairs MMP can spontaneously lead to robust ROS production and IL-1β release [42]. ROS, such as H_2O_2 and superoxide anions derived from mitochondria, can promote cytotoxicity and cell death, especially in disordered situations. Mitochondrial dysfunction and ROS production have been investigated in the initiation of cell death pathway signaling, such as the formation of NLRP3 inflammasomes, and in mediating subsequent GSDMD oligomerization and pore formation [43, 44]. Therefore, disrupted MMP and the subsequent accumulation of ROS play vital roles in macrophage NLRP3 inflammasome activation and pyroptosis. Transcriptome sequencing analysis revealed that BeG treatment regulated the expression of genes involved in mitochondrial translation and ROS metabolism in LPS- and ATP-stimulated BMDMs. Mitochondria lacking mtDNA or mitochondrial RNA granules accumulate ROS and have diminished membrane potential compared with those containing mtDNA or mitochondrial RNA granules [45]. Therefore, we examined the impact of BeG treatment on mitochondrial function. Our results showed that BeG treatment alleviated mitochondrial damage, reduced the accumulation of ROS induced by MMP depolarization, and regulated mitochondrial quality by promoting mitophagy, thus maintaining mitochondrial homeostasis. These findings reveal a potential treatment strategy for BeG in terms of immunity (pyroptosis) and metabolism (mitochondrial homeostasis).

Inhibition of mitophagy or autophagy by 3-MA leads to the accumulation of dysfunctional mitochondria and spontaneous activation of the NLRP3 inflammasome [42]. Genetic ablation of autophagy-related molecules ATG5 or Beclin 1 results in mitochondrial damage and accumulation of ROS, enhancing NLRP3 inflammasome activation during MSU or nigericin stimulation [42]. Therefore, we assessed whether the effects of BeG treatment on mitophagy and NLRP3 inflammasome activation might be causal. Consistent with previous studies, 3-MA reversed the inhibitory effects of BeG treatment on IL-1β release, cleaved caspase-1 release, LDH release, GSDMD-N formation, ROS production, and mRNA expression of *Il1b*, which suggests that BeG treatment suppresses NLRP3 inflammasome activation by promoting mitophagy. This explains how treatment with BeG regulates NLRP3 inflammasome activation and pyroptosis through intrinsic signals that reflect mitochondrial physiology. Fig. 7 depicts the signaling pathways through which BeG treatment sequentially mitigates NLRP3 inflammasome activation and pyroptosis.

To determine whether BeG inhibits inflammasome activation in vivo, NLRP3 inflammasome-dependent septic shock mouse models were used to explore the functional relevance of BeG treatment during NLRP3 activation. In this study, BeG treatment alleviated serum IL-1β production against bacterial infection, thereby increasing the survival of mice treated with a lethal dose of *E. coli*. *E. coli* mediated NLRP3 inflammasome activation triggers acute systemic inflammation in mice during sepsis [46, 47]. H&E staining revealed that BeG treatment significantly alleviated *E. coli* induced infiltration of inflammatory cells in the lungs, colon, and

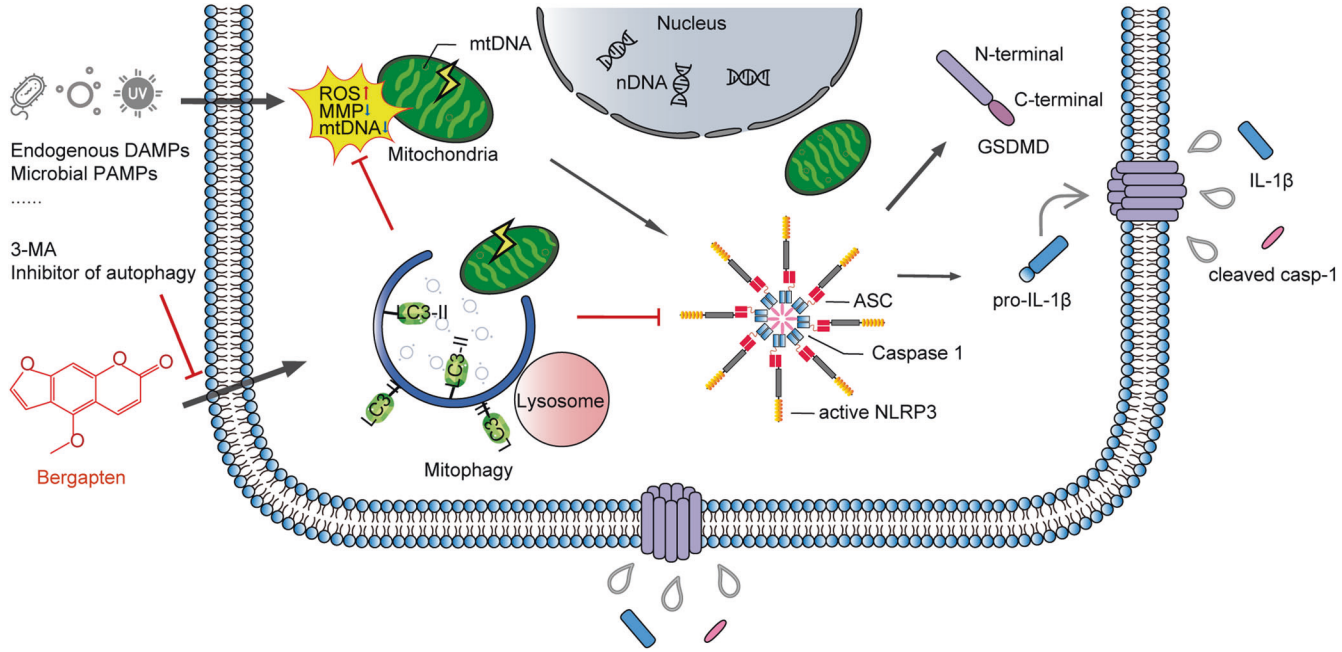

Fig. 7 Schematic representation of signaling pathways through which BeG treatment sequentially mitigates NLRP3 inflammasome activation and pyroptosis. BeG is a natural organic compound in herbal medicines which effectively inhibits NLRP3 inflammasome activation, IL-1β release, and pyroptosis through maintenance of mitochondrial homeostasis by promoting mitophagy.

liver of mice. Western blot showed that the treatment of BeG downregulated Casp1-P10 and GSDMD-N expression concomitantly with the induction of LC3 II in the lung following *E. coli* infection. These results demonstrated that BeG could inhibit NLRP3 inflammasome activation-related diseases to reduce inflammation. The mucosa of the intestine contains many resident macrophages in humans and mice [48, 49]. Macrophages are the gatekeepers of intestinal immune homeostasis that orchestrate innate and adaptive immune responses [50, 51]. Therefore, we investigated whether BeG treatment protects mice from *C. rodentium* induced intestinal inflammation. *C. rodentium* is a mouse pathogen that specifically activates the non-canonical NLRP3 inflammasome, resulting in potassium efflux and pyroptosis, subsequently causing NLRP3 inflammasome activation in macrophages [1, 52, 53]. *C. rodentium* induces cleaved-caspase-1 via the NLRP3 inflammasome in BMDMs [52]. Although we found that the activation of non-canonical NLRP3 was unaffected by BeG in vitro, inflammation induced by *C. rodentium* in mice was significantly attenuated by BeG treatment. Therefore, we speculate that the inhibitory effects of BeG on inflammation induced by *C. rodentium* not only depend on the inhibition of the NLRP3 inflammasome and pyroptosis but also rely on its antibacterial effect since a previous study has reported that BeG showed antibacterial activities against several bacterial isolates [54]. As an active ingredient in a wide range of medicinal plants, the effects of BeG on the NLRP3 inflammasome may add new insight into the therapeutic effects of these herbal medicines in addition to previously known benefits.

In summary, these findings collectively suggested that BeG treatment mitigated NLRP3 inflammasome activation and pyroptosis by promoting mitophagy. This study provides mechanistic insight into the immunomodulatory activity of BeG used in inflammatory diseases and suggests BeG as a potential anti-inflammatory drug for inflammatory diseases with dysregulated NLRP3 activation.

ACKNOWLEDGEMENTS

This work was supported by the National Natural Science Foundation (NNSF) of China (Nos. 82001663), Young Elite Scientists Sponsorship Program by China Association for Science and Technology (No. 2020-QNRC1-03), and Joint Fund of Beijing University of Traditional Chinese Medicine and USANA. We are grateful to Prof. Feng Shao (National Institute of Biological Sciences, Beijing, China) for providing iBMDM, Prof. Chen Dong (Tsinghua University, Beijing, China) for providing *C. rodentium*.

AUTHOR CONTRIBUTIONS

YW, XJ and ALX conceived the study; TL, WDF, JYW and FX performed the experiments. LDK, XJW, XL and RL contributed to the interpretation of results. TL and XJ wrote the manuscript and YW and ALX made pivotal revisions; YJC provided computational analysis; YW and ALX supervised the project.

ADDITIONAL INFORMATION

Supplementary information The online version contains supplementary material available at https://doi.org/10.1038/s41401-023-01094-7.

Competing interests: The authors declare no competing interests.

REFERENCES

1. Mangan MSJ, Olhava EJ, Roush WR, Seidel HM, Glick GD, Latz E. Targeting the NLRP3 inflammasome in inflammatory diseases. Nat Rev Drug Discov. 2018;17:588–606.
2. Lamkanfi M, Dixit VM. Inflammasomes and their roles in health and disease. Annu Rev Cell Dev Biol. 2012;28:137–61.
3. Broz P, Dixit VM. Inflammasomes: mechanism of assembly, regulation and signalling. Nat Rev Immunol. 2016;16:407–20.
4. Chen J, Chen ZJ. PtdIns4P on dispersed trans-Golgi network mediates NLRP3 inflammasome activation. Nature. 2018;564:71–76.
5. Shi J, Gao W, Shao F. Pyroptosis: Gasdermin-mediated programmed necrotic cell death. Trends Biochem Sci. 2017;42:245–54.
6. Bergsbaken T, Fink SL, Cookson BT. Pyroptosis: host cell death and inflammation. Nat Rev Microbiol. 2009;7:99–109.
7. Yu JW, Lee MS. Mitochondria and the NLRP3 inflammasome: physiological and pathological relevance. Arch Pharm Res. 2016;39:1503–18.
8. Zhong Z, Liang S, Sanchez-Lopez E, He F, Shalapour S, Lin X-J, et al. New mitochondrial DNA synthesis enables NLRP3 inflammasome activation. Nature. 2018;560:198–203.
9. Murakami T, Ockinger J, Yu J, Byles V, McColl A, Hofer AM, et al. Critical role for calcium mobilization in activation of the NLRP3 inflammasome. Proc Natl Acad Sci USA. 2012;109:11282–7.

10. Mishra SR, Mahapatra KK, Behera BP, Patra S, Bhol CS, Panigrahi DP, et al. Mitochondrial dysfunction as a driver of NLRP3 inflammasome activation and its modulation through mitophagy for potential therapeutics. Int J Biochem Cell Biol. 2021;136:106013.
11. Nakahira K, Haspel JA, Rathinam VAK, Lee SJ, Dolinay T, Lam HC, et al. Autophagy proteins regulate innate immune responses by inhibiting the release of mitochondrial DNA mediated by the NALP3 inflammasome. Nat Immunol. 2011;12:222–30.
12. Youle RJ, Narendra DP. Mechanisms of mitophagy. Nat Rev Mol Cell Biol. 2011;12:9–14.
13. Wu KKL, Long K, Lin H, Siu PMF, Hoo RLC, Ye D, et al. The APPL1-Rab5 axis restricts NLRP3 inflammasome activation through early endosomal-dependent mitophagy in macrophages. Nat Commun. 2021;12:6637.
14. Dagvadorj J, Mikulska-Ruminska K, Tumurkhuu G, Ratsimandresey RA, Carriere J, Andres AM, et al. Recruitment of pro-IL-1α to mitochondrial cardiolipin, via shared LC3 binding domain, inhibits mitophagy and drives maximal NLRP3 activation. Proc Natl Acad Sci USA. 2021;118:e2015632118.
15. Borgatti M, Mancini I, Bianchi N, Guerrini A, Lampronti I, Rossi D, et al. Bergamot (*Citrus bergamia* Risso) fruit extracts and identified components alter expression of interleukin 8 gene in cystic fibrosis bronchial epithelial cell lines. BMC Biochem. 2011;12:15.
16. Chen G, Xu Q, Dai M, Liu X. Bergapten suppresses RANKL-induced osteoclastogenesis and ovariectomy-induced osteoporosis via suppression of NF-κB and JNK signaling pathways. Biochem Biophys Res Commun. 2019;509:329–34.
17. Liang Y, Xie L, Liu K, Cao Y, Dai X, Wang X, et al. Bergapten: a review of its pharmacology, pharmacokinetics, and toxicity. Phytother Res. 2021;35:6131–47.
18. Adakudugu EA, Ameyaw EO, Obese E, Biney RP, Henneh IT, Aidoo DB, et al. Protective effect of bergapten in acetic acid-induced colitis in rats. Heliyon. 2020;6:e04710.
19. Adakudugu EA, Obiri DD, Ameyaw EO, Obese E, Biney RP, Aidoo DB, et al. Bergapten modulates ovalbumin-induced asthma. Sci African. 2020;8:e00457.
20. Aidoo DB, Obiri DD, Osafo N, Antwi AO, Essel LB, Duduyemi BM, et al. Allergic airway-induced hypersensitivity is attenuated by bergapten in murine models of inflammation. Adv Pharm Sci. 2019;2019:6097349.
21. Zhou Y, Wang J, Yang W, Qi X, Lan L, Luo L, et al. Bergapten prevents lipopolysaccharide-induced inflammation in RAW264.7 cells through suppressing JAK/STAT activation and ROS production and increases the survival rate of mice after LPS challenge. Int Immunopharmacol. 2017;48:159–68.
22. Pan H, Lin Y, Dou J, Fu Z, Yao Y, Ye S, et al. Wedelolactone facilitates Ser/Thr phosphorylation of NLRP3 dependent on PKA signalling to block inflammasome activation and pyroptosis. Cell Prolif. 2020;53:e12868.
23. Zhu X, Zhang HW, Chen HN, Deng XJ, Tu YX, Jackson AO, et al. Perivascular adipose tissue dysfunction aggravates adventitial remodeling in obese mini pigs via NLRP3 inflammasome/IL-1 signaling pathway. Acta Pharmacol Sin. 2019;40:46–54.
24. Feng WD, Wang Y, Luo T, Jia X, Cheng CQ, Wang HJ, et al. Scoparone suppresses mitophagy-mediated NLRP3 inflammasome activation in inflammatory diseases. Acta Pharmacol Sin. 2022. https://doi.org/10.1038/s41401-022-01028-9. Online ahead of print.
25. Swanson KV, Deng M, Ting JPY. The NLRP3 inflammasome: molecular activation and regulation to therapeutics. Nat Rev Immunol. 2019;19:477–89.
26. Lu A, Magupalli VG, Ruan J, Yin Q, Atianand MK, Vos MR, et al. Unified polymerization mechanism for the assembly of ASC-dependent inflammasomes. Cell. 2014;156:1193–206.
27. Frank D, Vince JE. Pyroptosis versus necroptosis: similarities, differences, and crosstalk. Cell Death Differ. 2019;26:99–114.
28. Bronner DN, Abuaita BH, Chen X, Fitzgerald KA, Nuñez G, He Y, et al. Endoplasmic reticulum stress activates the inflammasome via NLRP3- and Caspase-2-driven mitochondrial damage. Immunity. 2015;43:451–62.
29. Jo EK, Kim JK, Shin DM, Sasakawa C. Molecular mechanisms regulating NLRP3 inflammasome activation. Cell Mol Immunol. 2016;13:148–59.
30. Quiros PM, Goyal A, Jha P, Auwerx J. Analysis of mtDNA/nDNA ratio in mice. Curr Protoc Mouse Biol. 2017;7:47–54.
31. Kampira E, Dzobo K, Kumwenda J, van Oosterhout JJ, Parker MI, Dandara C. Peripheral blood mitochondrial DNA/nuclear DNA (mtDNA/nDNA) ratio as a marker of mitochondrial toxicities of stavudine containing antiretroviral therapy in HIV-infected Malawian patients. OMICS. 2014;18:438–45.
32. Dan Dunn J, Alvarez LA, Zhang X, Soldati T. Reactive oxygen species and mitochondria: a nexus of cellular homeostasis. Redox Biol. 2015;6:472–85.
33. Brookes PS, Yoon Y, Robotham JL, Anders MW, Sheu SS. Calcium, ATP, and ROS: a mitochondrial love-hate triangle. Am J Physiol Cell Physiol. 2004;287:C817–C833.
34. Ashrafi G, Schwarz TL. The pathways of mitophagy for quality control and clearance of mitochondria. Cell Death Differ. 2013;20:31–42.
35. Tanida I, Ueno T, Kominami E. LC3 conjugation system in mammalian autophagy. Int J Biochem Cell Biol. 2004;36:2503–18.
36. von Moltke J, Ayres JS, Kofoed EM, Chavarría-Smith J, Vance RE. Recognition of bacteria by inflammasomes. Annu Rev Immunol. 2013;31:73–106.
37. Huang Y, Xu W, Zhou R. NLRP3 inflammasome activation and cell death. Cell Mol Immunol. 2021;18:2114–27.
38. Wang K, Sun Q, Zhong X, Zeng M, Zeng H, Shi X, et al. Structural mechanism for GSDMD targeting by autoprocessed caspases in pyroptosis. Cell. 2020;180:941–55.e20.
39. Shen C, Zhang Z, Xie T, Xu J, Yan J, Kang A, et al. Jinxin oral liquid inhibits human respiratory syncytial virus-induced excessive inflammation associated with blockade of the NLRP3/ASC/Caspase-1 pathway. Biomed Pharmacother. 2018;103:1376–83.
40. Seoane PI, Lee B, Hoyle C, Yu S, Lopez-Castejon G, Lowe M, et al. The NLRP3-inflammasome as a sensor of organelle dysfunction. J Cell Biol. 2020;219:e202006194.
41. Abais JM, Xia M, Zhang Y, Boini KM, Li PL. Redox regulation of NLRP3 inflammasomes: ROS as trigger or effector? Antioxid Redox Signal. 2015;22:1111–29.
42. Zhou R, Yazdi AS, Menu P, Tschopp J. A role for mitochondria in NLRP3 inflammasome activation. Nature. 2011;469:221–5.
43. Próchnicki T, Latz E. Inflammasomes on the crossroads of innate immune recognition and metabolic control. Cell Metab. 2017;26:71–93.
44. Evavold CL, Hafner-Bratkovič I, Devant P, D'Andrea JM, Ngwa EM, Boršić E, et al. Control of gasdermin D oligomerization and pyroptosis by the Ragulator-Rag-mTORC1 pathway. Cell. 2021;184: 4495–511.e19.
45. Kleele T, Rey T, Winter J, Zaganelli S, Mahecic D, Perreten Lambert H, et al. Distinct fission signatures predict mitochondrial degradation or biogenesis. Nature. 2021;593:435–9.
46. Dufies O, Doye A, Courjon J, Torre C, Michel G, Loubatier C, et al. Escherichia coli Rho GTPase-activating toxin CNF1 mediates NLRP3 inflammasome activation via p21-activated kinases-1/2 during bacteraemia in mice. Nat Microbiol. 2021;6:401–12.
47. Liu Y, Jing YY, Zeng CY, Li CG, Xu LH, Yan L, et al. Scutellarin suppresses NLRP3 inflammasome activation in macrophages and protects mice against bacterial sepsis. Front Pharmacol. 2017;8:975.
48. Bull DM, Bookman MA. Isolation and functional characterization of human intestinal mucosal lymphoid cells. J Clin Invest. 1977;59:966–74.
49. Delfini M, Stakenborg N, Viola MF, Boeckxstaens G. Macrophages in the gut: masters in multitasking. Immunity. 2022;55:1530–48.
50. Na YR, Stakenborg M, Seok SH, Matteoli G. Macrophages in intestinal inflammation and resolution: a potential therapeutic target in IBD. Nat Rev Gastroenterol Hepatol. 2019;16:531–43.
51. Zhang Q, Chen LH, Yang H, Fang YC, Wang SW, Wang M, et al. GPR84 signaling promotes intestinal mucosal inflammation via enhancing NLRP3 inflammasome activation in macrophages. Acta Pharmacol Sin. 2022;43:2042–54.
52. Liu Z, Zaki MH, Vogel P, Gurung P, Finlay BB, Deng W, et al. Role of inflammasomes in host defense against Citrobacter rodentium infection. J Biol Chem. 2012;287:16955–64.
53. Kayagaki N, Warming S, Lamkanfi M, Vande Walle L, Louie S, Dong J, et al. Non-canonical inflammasome activation targets caspase-11. Nature. 2011;479:117–21.
54. Aldulaimi O. Screening of fruits of seven plants indicated for medicinal use in Iraq. Pharmacogn Mag. 2017;13:S189–S195.